

## CFD MODELLING OF ISOTHERMAL MULTIPLE JETS IN A COMBUSTOR

Shen LONG<sup>1\*</sup>, Zhao Feng TIAN, Graham NATHAN, Alfonso CHINNICI, Bassam DALLY

<sup>1</sup> School of Mechanical Engineering, The University of Adelaide, South Australia 5005, Australia

\*Corresponding author, E-mail address: shen.long@adelaide.edu.au

### ABSTRACT

This paper assesses the performance of three turbulence models on the simulation of an isothermal flow from a burner with three separated-jet inlets. This burner has key flow features of a novel hybrid solar receiver combustor (HSRC) that is under development in the Centre for Energy Technology (CET) at the University of Adelaide. Three turbulence models, namely, the Baseline Reynolds Stress (BSL RSM), the Shear-Stress-Transport (SST) and the Standard k- $\epsilon$  (SKE) models were chosen. The paper reports numerical results from two cases of the separated-jet flows. In these two cases, the angle between the side jet and the centre jet is 0° and 20°. The predicted mean velocity profiles at six positions of this burner are compared against experimental results from the literature. It is found that the best prediction is provided by the BSL RSM model, which predicts well the velocity peaks and reproduces the trend of velocity profiles in different axial positions. Importantly, the BSL RSM model has the advantage of predicting anisotropic Reynolds stresses in interacting jet flows. This opens the way to use these models to inform the development of the combustion system within the HSRC.

### INTRODUCTION

The concept of integrating Concentrating Solar Thermal (CST) technology and traditional combustion energy is gaining prominence globally due to the complementary nature of these two thermal energy sources (Ordorica-Garcia, Delgado & Garcia 2011). CST can reduce the emission of greenhouse gas and provide a cost-effective way to incorporate solar with thermal energy storage (Steinmann 2012) to overcome the challenge of the intermittent nature of solar radiation (Jin & Hong 2012). The integration of combustion energy source with CST offers a relatively low cost solution which minimises the need for costly long term energy storage and provides certainty for baseload power.

A Hybrid Solar Receiver Combustor (HSRC) has been proposed by the Centre for Energy Technology (CET) at the University of Adelaide, which is a combination of a solar cavity receiver and a gaseous fuel combustor. The HSRC reduces heat losses relative to equivalent hybrids by integrating CST and combustion energy source into a single device (Nathan et al. 2013; Nathan et al. 2009). The HSRC is designed to operate in any of three modes: the 'combustion only mode', the 'solar only mode' and the 'mixed mode'. For the 'solar only mode', the shutter of Compound Parabolic Concentrator (CPC) is open to allow the entry of concentrated solar radiation into the receiver, so that the heat source for the HSRC is only solar energy. In contrast, the heat source in the 'combustion only mode'

is derived only from the burning of injected fuel. In the 'mixed mode', the heat source for the HSRC is derived from both solar radiation and combustion, with the percentage of each being dependent on the solar intensity available at the time. A schematic diagram of the HSRC is presented in Figure 1.

The HSRC is still in the early stages of development. Owing to the range of operational modes, it can be expected that different flow regimes, flame structures and dominant heat transfer mechanisms will occur at different times inside the HSRC. Hence there is a need to understand the flow dynamics of this unique geometry to design burners that can work effectively. Based on the proposed configurations of the HSRC, multiple burners are distributed within the conical configuration of the chamber with an angle of inclination ( $\beta_{jet}$ ) that causes the jets to interact within the chamber (Figure 1). According to Chinnici (2015), by changing the inclination angle of the jet from 30° to 90°, the flow features and combustion behaviours inside the HSRC change dramatically. Therefore, a comprehensive understanding of the influence of interacting jets on flow dynamics inside the HSRC is desirable.

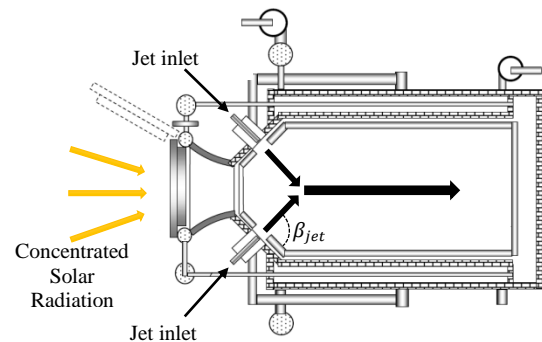
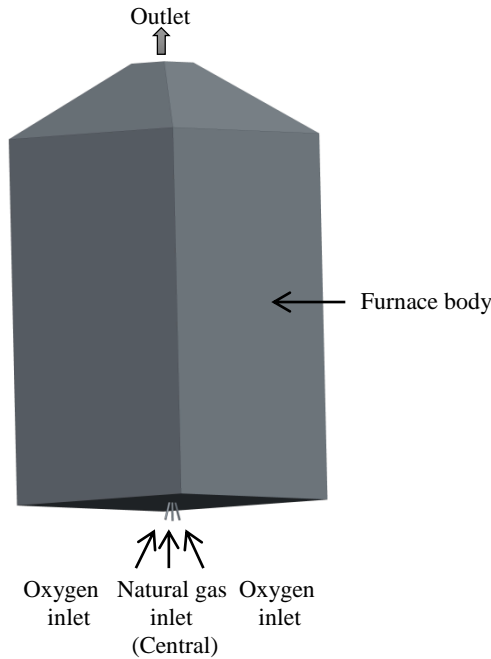


Figure 1: Schematic diagram of the Hybrid Solar Receiver Combustor (Nathan et al. 2013).

Prior to building experimental facilities with which to directly assess the performance of the HSRC, CFD models have been developed using other experimental data from related configurations. Of these, the investigation of interacting jets of an oxy-fuel combustion separated-jet burner developed by Boushaki and Sautet (2010) was chosen for CFD model validation. This burner consists of a central jet of natural gas placed between two oxygen jets, the orientation of which is adjustable (Boushaki et al. 2008; Boushaki et al. 2007). Hence this system has similar features to the multiple-jet configuration of the HSRC. A schematic diagram of this system is shown in Figure 2. Importantly, the work of Boushaki and Sautet (2010)

provides sufficient details of the geometry and flow velocity measurement for reliable model development and validation.



**Figure 2:** Schematic diagram of the separated-jet burner of Boushaki and Sautet (2010).

In light of the needs mentioned above, the aim of the present paper is to conduct a CFD study to better understand the flow behaviour of inclined jets and to test the performance of different turbulence models in predicting the flow behaviour of a separated-jet burner. The performance of three turbulence models, namely, the Baseline Reynolds Stress (BSL RSM) model, Standard  $k-\epsilon$  (SKE) model and Shear-Stress-Transport (SST) model, is evaluated in this study. The selection of these models was based on our previous CFD modelling studies of flows in a solar-enhanced vortex gasifier (Tian, Nathan & Cao 2015). Particularly, this study compares the simulated results against the experimental data of axial velocity

profiles at six positions from the burner exit, in non-reacting conditions.

## MODEL DESCRIPTION

The computational model of the separated-jet burner shown in Figure 3 was generated with a commercial CAD package Creo 2.0. Two models of the burner have been constructed for the case of  $\alpha_{jet} = 0^\circ$  and  $\alpha_{jet} = 20^\circ$ . The dimensions of the burner are shown in Table 1.

The ANSYS/ICEM CFD code was used to generate the structural mesh of this computational model. In order to accelerate the process of mesh generation and refinement, the shape of the burner has been simplified by replacing the conical structure of the exhaust duct (Figure 2) with a square structure (Figure 3). While this change will inevitably influence the secondary flows in the chamber, here our primary interest is the first order recirculation flow patterns. Additionally, due to the symmetric configuration of this burner, only a quarter of the full domain was analysed and a symmetric boundary was employed. This results in an efficient use of the number of mesh nodes. The mesh quality was checked for expansion factor, aspect ratio, skewness and orthogonality. The influence of the number of mesh nodes on the CFD results was evaluated through a mesh independence test, which is reported in the next section.

The flow field measurements reported by Boushaki and Sautet (2010) were undertaken by replacing natural gas with an inert mixture of 65.38% of nitrogen and 34.63% of helium (by volume) to achieve a similar density to natural gas. Hence in this paper the designation of ‘central jet’ is used to denote the mixed gases in this jet. The mass flow rate of the central jet and oxygen jet were held constant for all simulation cases to match the inlet conditions in the reference paper of Boushaki and Sautet (2010). The detailed boundary conditions are given in Table 2 and 3, and the complete boundary settings and experimental configurations are reported by Boushaki and Sautet (2010).

The CFD calculations were carried out with the commercial Finite Volume code ANSYS CFX 16.1. The convergence criterion for all simulations was set to be  $1 \times 10^{-5}$  (RMS).

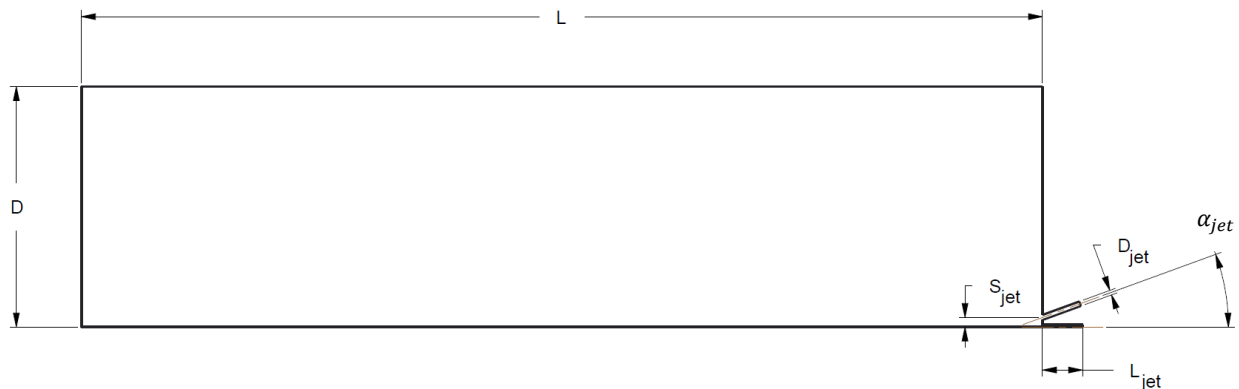


**Figure 3:** Geometry of the CFD domain.

Dimension	Description	Value (mm)
<b>D</b>	Furnace width (half)	300
<b>L</b>	Furnace length	1200
$L_{jet}$	Jet inlet length	50
$S_{jet}$	Distance between jets	12
$D_{jet}$	Jet diameter	6
$\alpha_{jet}$	Jet inclination angle	0° and 20°

**Table 1:** Geometric parameters.

Boundary Type	Mass Flow Rate (kg/s)
Central Inlet	0.000556
Oxygen Inlet	0.001964

**Table 2:** Inlet boundary details.

Boundary Name	Boundary Type
1,2	Mass flow inlet
3	Opening
4	Symmetric planes
Other	No slip wall

**Table 3:** Boundary conditions.

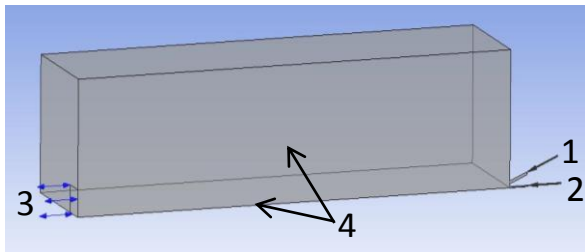


**Figure 4:** CFD Domain

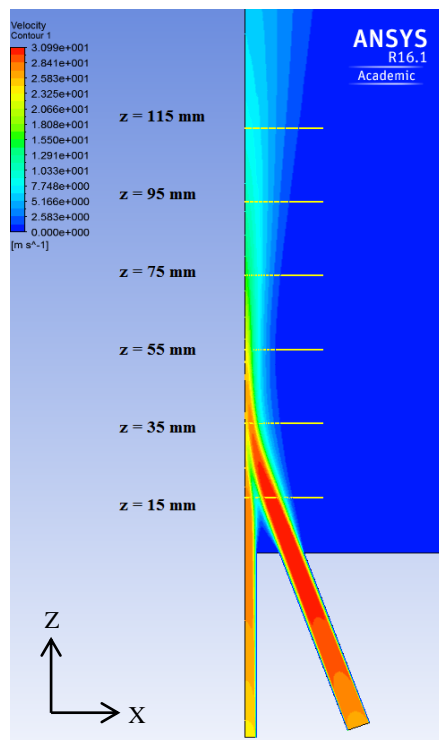


**Figure 5:** The six measurement planes, together with the mean velocity profile simulated by 4 million mesh nodes with  $\alpha_{jet} = 20^\circ$ .

## RESULTS

### Mesh independence test

A series of mesh refinements was carried out for four different grid sizes of 1 million, 2 million, 4 million and 8 million mesh nodes, respectively. The BSL RSM model was chosen to investigate the influence of the number of mesh nodes on the results, for the case with  $\alpha_{jet} = 20^\circ$ . In the work of Boushaki and Sautet (2010), the mean axial velocity profiles were obtained at six radial traverses at the axial locations of  $z = 15$  mm, 35 mm, 55 mm, 75 mm, 95 mm, 115 mm, as is illustrated in Figure 5. The comparison between the numerical results and experimental data at  $z = 15$  mm and 115 mm is shown in Figure 6. At  $z = 15$  mm (Figure 6 a), it can be seen that there is only a slight difference between the results predicted using these four mesh sizes, and all simulated results are similar to experimental data. At  $z = 115$  mm (Figure 6 b), the prediction also changes little with an increase in the number of mesh nodes, although all models under-predict the velocity profile. This under-prediction may be caused by the inaccurate reproduction of an out-of-plane motion as the mass flow and momentum are conserved. Therefore, 4 million mesh size was chosen to evaluate the performance of turbulence models in this study.

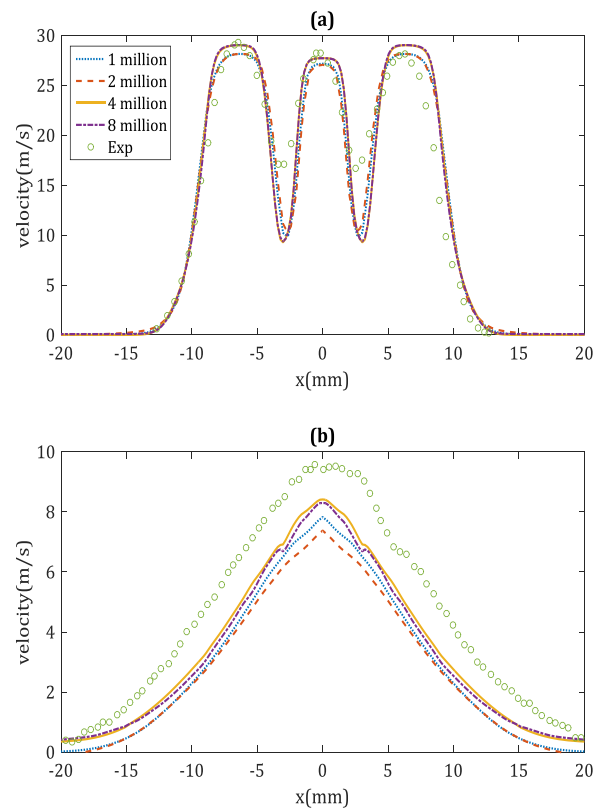


**Figure 6:** Comparison between the CFD simulations and the experiments for four different mesh sizes at (a)  $z = 15$  mm and (b)  $z = 115$  mm.

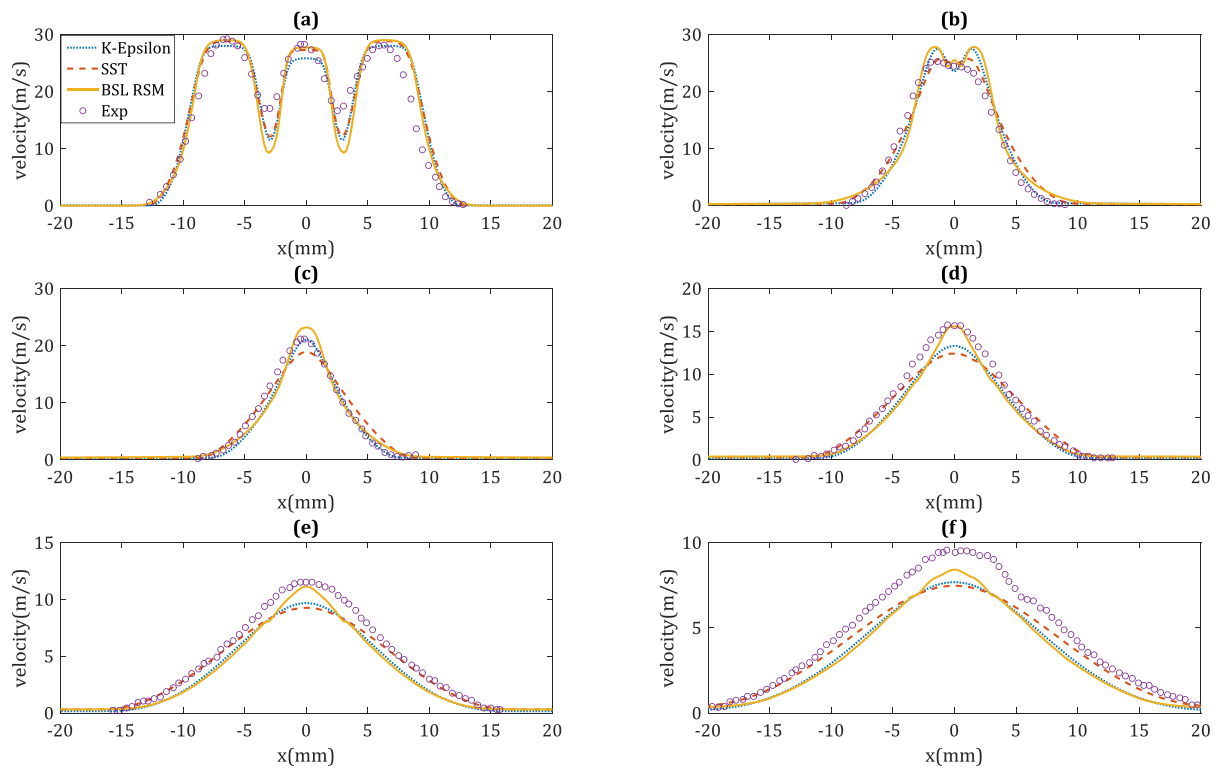


**Figure 7:** Comparison of calculated radial profile of mean axial velocity using three turbulence models with experimental data  $\alpha_{jet} = 20^\circ$  (Boushaki & Sautet 2010) at axial positions (a)  $z = 15$  mm, (b)  $z = 35$  mm, (c)  $z = 55$  mm, (d)  $z = 75$  mm, (e)  $z = 95$  mm, (f)  $z = 115$  mm.

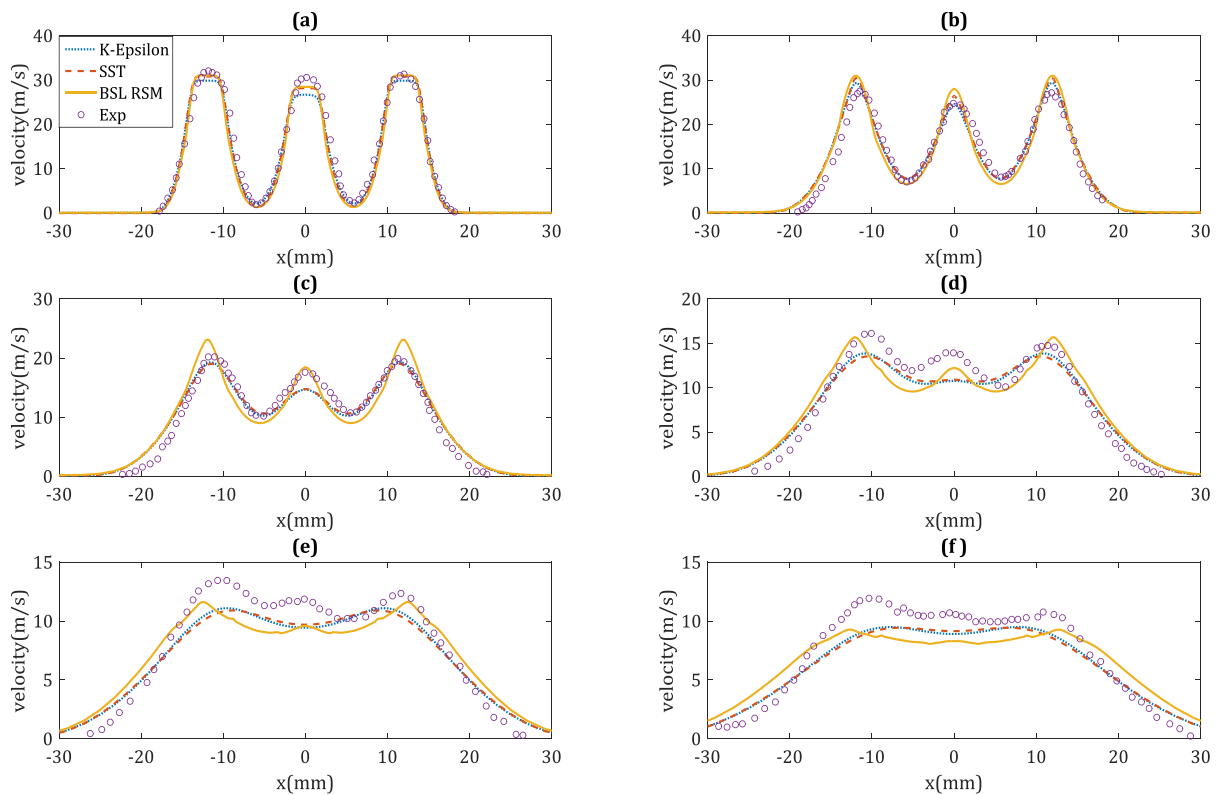


**Figure 8:** Comparison of calculated radial profile of mean axial velocity using three turbulence models with experimental data  $\alpha_{jet} = 0^\circ$  (Boushaki & Sautet 2010) at axial positions (a)  $z = 15$  mm, (b)  $z = 35$  mm, (c)  $z = 55$  mm, (d)  $z = 75$  mm, (e)  $z = 95$  mm, (f)  $z = 115$  mm.

### Comparison of different turbulence models

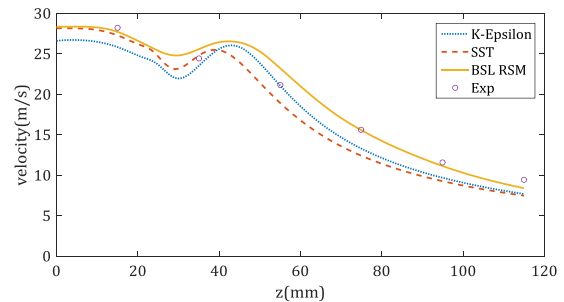
Figure 7 shows the comparison of mean axial velocity profiles at six positions downstream from the burner exit ( $z = 15$  mm, 35 mm, 55 mm, 75 mm, 95 mm and 115 mm) to illustrate the performance of different turbulence models for the case of  $\alpha_{jet} = 20^\circ$ . At  $z = 15$  mm (Figure 7 a), all turbulence models provide good agreement with the experimental data for the side jets (oxygen jets shown in Figure 2), while they under-predict the velocity at the central jets (maximum difference 5%). Similarly, at  $z = 35$  mm (Figure 7 b), all three models slightly over-predict the peak value of velocity by about 5% ( $x = \pm 12$  mm, 0 mm), and results of the SKE model are in relatively good agreement with the experimental data. However, at  $z = 55$  mm (Figure 7 c), the predictions based on BSL RSM model have a similar trend to the SKE model, while they over-predict the velocity magnitude around the central jet region (maximum difference 8% at  $x = 0$  mm). At  $z = 75$  mm (Figure 7 d), the jet velocity predicted by the BSL RSM model is quite similar to that of the measurement, which reproduces the peak velocity at  $x = 0$  mm. Also, at  $z = 95$  mm (Figure 7 e), the maximum value of under-prediction is found to be 19.5% at  $x = 0$  mm, which is provided by the SST model. The jet velocity predicted by the BSL RSM model at the centre of the jet ( $x = 0$  mm) has the best agreement with the experimental data. In addition, at  $z = 115$  mm (Figure 7 f), all models under-predict the velocity value at all jet regions, while the results from BSL RSM model agree best with the measured data at  $x = 0$  mm, where there is 10% difference between the measured and calculated velocity.

Figure 8 presents a comparison of the mean axial velocity profiles at the same six positions from the burner exit for the case of  $\alpha_{jet} = 0^\circ$ . At  $z = 15$  mm (Figure 8 a), the maximum difference occurs at  $x = 0$  mm, the SKE model under-predicts the velocity by about 11.5%, the SST model by 6.5% and the BSL RSM model by 5.5%. Also, at  $z = 35$  mm (Figure 8 b), all models slightly over-predict the velocity magnitude in the three jet regions. At  $z = 55$  mm (Figure 8 c), the BSL RSM model offers a good match with the central velocity peak, but an obvious difference to the side velocity peaks (around 10%). At  $z = 75$  mm (Figure 8 d), the results based on all three models are slightly different from the experimental data. The SKE model and the SST model can only reproduce the trends in the velocity of the two side jets, while the predictions of the central jet velocity profile differ significantly from the data. A closer observation indicates that the simulated velocity profile from the BSL RSM model agrees best with the experimental data since it reproduces all three peak velocity regions. At  $z = 95$  mm (Figure 8 e) and  $z = 115$  mm (Figure 8 f), there are significant differences between the numerical results and the experimental data for all tested turbulence models. Notably, the results of BSL RSM model under-predict most of the measured locations between  $z = 95$  mm and 115 mm. However, this model still reproduces the velocity trend for all three velocity peaks, and the overall trend is in reasonable agreement with that of the experiment.

### Discussion

Generally, reasonable agreement with the measured data can be obtained using all three turbulence models for the case of  $\alpha_{jet} = 0^\circ$  and  $20^\circ$ . Both SKE and SST models under-predict the jets downstream the location  $z = 75$  mm

(maximum difference 20.5%). This under-prediction is consistent with their performance in modelling a single round free jet. For instance, Figure 9 shows the centreline velocity decay of the central jet for the case of  $\alpha_{jet} = 20^\circ$ . It can be seen that the velocity decay of SKE and SST models is much higher than that of BSL RSM model, and BSL RSM model provides good agreement with the experimental data at  $z = 15$  mm, 75 mm, 95 mm and 115 mm.



**Figure 9:** Comparison of centreline velocity decay of the central jet using three turbulence models with experimental data  $\alpha_{jet} = 20^\circ$  (Boushaki & Sautet 2010) along the  $z$  axis.

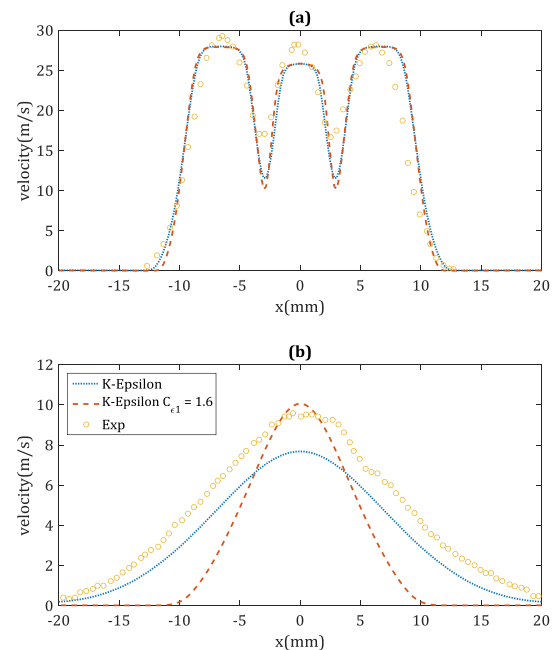


**Figure 10:** Comparison of calculated radial profile of mean axial velocity from two different  $C_{\epsilon 1}$  at axial positions (a)  $z = 15$  mm, (b)  $z = 115$  mm with experimental data (Boushaki & Sautet 2010).

Specifically, it is well known that the SKE model over-predicts the velocity decay of a round free jet. Morse (1980) and Pope (1978) suggested to change the constant  $C_{\epsilon 1}$  (Epsilon coefficient) in the turbulence dissipation rate,  $\epsilon$ , equation of the SKE model from 1.44 to 1.6, to overcome the under-prediction of a round free jet. Figure 10 illustrates the simulated mean axial velocity profile from two different  $C_{\epsilon 1}$  values at  $z = 15$  mm and  $z = 115$  mm. It can be seen that at the upstream region ( $z = 15$  mm), there is no significant difference between the results from the two  $C_{\epsilon 1}$  values. However, in the far-field region ( $z = 115$  mm), changing the value of  $C_{\epsilon 1}$  to 1.6 only

provides a good prediction for central jet, but under-predicts the side jets compared with the default value of  $C_{\epsilon 1}$  (1.44). Hence, this change does not improve the simulated results in these cases.

The performance of the BSL RSM model is slightly better than that of SST and SKE models. According to Tian, Nathan and Cao (2015), the normal Reynolds stress in both SKE model and SST model are assumed to be isotropic, which reduces the prediction accuracy of a turbulence model when dealing with turbulence flow conditions such as jet interaction. By resolving turbulence intensity and additional transport equations, the BSL RSM model considers the anisotropic Reynolds stresses. Figure 11 shows the predicted normal Reynolds stress of BSL RSM model at  $z = 115$  mm,  $\alpha_{jet} = 20^\circ$ . The normal Reynolds stress  $\tau_{ww}$  (ww in the figure) is predicted to be much higher than the normal Reynolds stress  $\tau_{vv}$  and  $\tau_{uu}$ . This may explain why the BSL RSM model has a better performance of predicting interacting jet flow than the other two models.

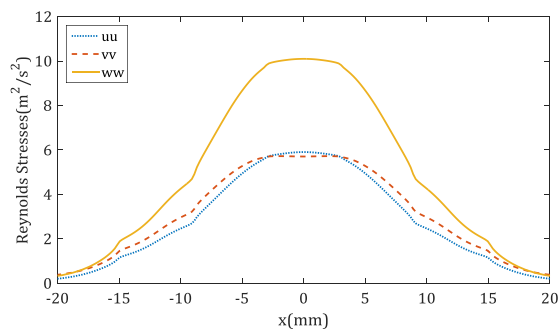


**Figure 11:** Predicted Reynolds stresses of BSL RSM model at  $z = 115$  mm with  $\alpha_{jet} = 20^\circ$ .

## CONCLUSION

The simulated results of the Baseline Reynolds Stress (BSL RSM), the Standard  $k-\epsilon$  (SKE) and the Shear-Stress-Transport (SST) models were found to predict the experimental data reasonably well at upstream locations of  $z = 15$  mm to  $z = 55$  mm in Boushaki and Sautet (2010), where  $z$  is the downstream distance from the burner exit. However, all three models under-predict the measured velocity for locations  $z = 75$  mm to  $115$  mm. The best model is the BSL RSM model, which predicts the peak velocity magnitude ( $z = 75$  mm) and reproduces the trend of velocity profiles in different axial positions. Owing to the advantage of predicting the anisotropic Reynolds stresses, the BSL RSM model mitigates the deficiency found in SKE and SST models. Therefore, the BSL RSM model is expected to provide good prediction to interacting jet flows, and it is deduced to be the preferred type of RANS model for the turbulent flows inside the HSRC.

## ACKNOWLEDGEMENTS

The authors will acknowledge the financial support from the Australian Research Council.

## REFERENCES

BOUSHAKI, T., MERGHENI, M.A., SAUTET, J.C., LABEGORRE, B (2008), "Effects of inclined jets on

turbulent oxy-flame characteristics in a triple jet burner", *Exp. Therm. Flu. Sci.*, **32**, 1363-1370.

BOUSHAKI, T., SAUTET, J., SALENTEY, L., LABEGORRE, B (2007), "The behaviour of lifted oxy-fuel flames in burners with separated jets", *Int. Commun. Heat Mass*, **34**, 8-18.

BOUSHAKI, T. and SAUTET, J.C. (2010), "Characteristics of flow from an oxy-fuel burner with separated jets: influence of jet injection angle", *Exp. Fluids*, **48**, 1095-1108.

CHINNICI, A. (2015), Internal Report. The University of Adelaide, School of Mechanical Engineering.

JIN, H.G., HONG, H. (2012), "12 - Hybridization of concentrating solar power (CSP) with fossil fuel power plants", in K Lovegrove & W Stein (eds), *Concentrating Solar Power Technology*, Woodhead Publishing, 395-420.

MORSE, A.P. (1980), "Axisymmetric Turbulent Shear Flows with and Without Swirl", *Thesis*, University of London.

NATHAN, G.J., DALLY, B., ASHMAN, P., STEINFELD, A., (2013), "A hybrid receiver-combustor", Provisional Patent Application No. 2012/901258., Adelaide Research and Innovation Pty. Ltd.; 2012 [Priority Date: 29.03.2].

NATHAN, G.J., HU, E.J., DALLY, B., ALWAHABI, Z., BATTYE, D.L., ASHMAN, P. (2009), 'A boiler system receiving multiple energy sources', Provisional Patent Application No.2009/905065 [Priority Date: 19.10.09].

ORDORICA-GARCIA, G., DELGADO, A.V., GARCIA, A.F. (2011), "Novel integration options of concentrating solar thermal technology with fossil-fuelled and CO<sub>2</sub> capture processes", *Energy Procedia*, **4**, 809-816.

POPE, S.B. (1978), "An explanation of the turbulent round-jet/plane-jet anomaly", *AIAA. J.*, **16**, 279-281.

STEINMANN, W.D. (2012), "11 - Thermal energy storage systems for concentrating solar power (CSP) plants", in K Lovegrove & W Stein (eds), *Concentrating Solar Power Technology*, Woodhead Publishing, 362-394.

TIAN, Z.F., NATHAN, G.J., CAO, Y. (2015), "Numerical modelling of flows in a solar-enhanced vortex gasifier: Part 1, comparison of turbulence models", *Prog. Comput. Fluid Dy.*, **15**, 114-122.